

3D Magneto-Thermal Computations in Induction Heating. Models and Experimental Validations

Bernard PAYA, Virgiliu FIRETEANU, Alexandru SPAHIU, Christophe GUERIN

Abstract— This paper presents the results of a series of tests made in order to validate the Magneto-Thermal module of the new FLUX3D v. 8.1. The tool was conceived to solve the coupled problems of electromagnetic and thermal phenomena. The solving method of the program considers a Thermal-Transient problem during a certain period of time and it solves, at each time step, the thermal and electromagnetic equations (in steady state Magneto-harmonic formulation), alternatively. We have modelled the inductive longitudinal welding of steel pipes. The results of 3D simulations are compared with measurements on a laboratory device.

Index Terms—Coupled problems, Magneto-thermal computation, Experimental validation

I. INTRODUCTION

Today, many industrial applications use electromagnetic induction as an energetically efficient way for heating and processing electrical conductive materials. By nature, there is a strong connection between the electromagnetic and thermal phenomena, which forces us to take into consideration the dependency of the electromagnetic (ρ , μ_r) and thermal (λ , ρC_p) properties on temperature. This means that we have to solve, what is called, coupled problems [1], [2]. Especially, we are interested in modelling the behaviour of materials around critical points like Curie.

This paper presents news developments in 3D magneto-thermal computation available in the version 8.1 of the software FLUX3D. It allows to simulate the evolution of electromagnetic and thermal phenomena during an induction heating process, either by a linking from a magneto-harmonic resolution to a transient thermal one, or by a weak coupling between the two resolutions. We have performed some experimental validations for a medium frequency (MF) and a high frequency (HF) induction heating application and we have compared their results with the computed ones.

Manuscript received September 6, 2002.

B. PAYA is with Électricité de France, R & D Centre des Renardières, F-77818 Morêt sur Loing Cedex, France. (e-mail : bernard.paya@edf.fr)

V. FIRETEANU and A. SPAHIU are with POLITEHNICA University, EPM Laboratory, 313 Spl. Independentei, Bucharest, Romania. (e-mail: firetean@electro.masuri.pub.ro)

C. GUERIN is with CEDRAT, 10 Chemin du Pré Carré – ZIRST F-38246 Meylan Cedex. (e-mail : christophe.guerin@cedrat.com)

II. NUMERICAL MODELS FOR MAGNETO-THERMAL COMPUTATIONS

A. magneto-harmonic model

Many magneto-harmonic models are available in the FLUX3D software. We have demonstrated in [3] that, for induction heating applications, the $T\Phi$ - Φ / Φ red model of the electromagnetic field is the most efficient in term of used memory and computation time. This model uses $T\Phi$ formulation in eddy current regions (conductive, magnetic or non-magnetic regions), Φ formulation in magnetic and non-conductive regions and Φ red formulation in non-magnetic and non-conductive regions. The equations solved in eddy current regions are :

$$\begin{aligned} -\overrightarrow{\text{curl}}(\rho \overrightarrow{\text{curl}} T) + \overrightarrow{\text{grad}}(\rho \text{div} T) + j\omega\mu(-\overrightarrow{T} + \overrightarrow{\text{grad}}\Phi) &= 0 \\ -\text{div}(\mu(\overrightarrow{T} - \overrightarrow{\text{grad}}\Phi)) &= 0 \end{aligned} \quad (1)$$

where the resistivity ρ and the magnetic permeability μ may depend on the temperature θ . When studying the induction heating of ferrous pieces, we must also take into account the magnetic field dependence of the magnetic permeability, because the correspondent regions are often very saturated. Since the electrical period is very small compared with the thermal time step, the time average volume power density dissipated in the conductive regions represents the source of the thermal problem.

For small skin depth (δ) problems, i. e. high frequency applications, it may be useful to introduce the surface impedance (Z_s) formulation [4] on the surface between the conductive and the non conductive region as :

$$\vec{n} \times \vec{E} = Z_s \vec{n} \times (\vec{n} \times \vec{H}) \quad (2)$$

where Z_s may be evaluated, for linear problems, as :

$$Z_s = (1 + j) \frac{\rho}{\delta} \quad (3)$$

In this case, the power dissipated by eddy currents is a

surface power density that appears like a thermal flux density on the surface of the eddy current region.

Some non linear models of surface impedance have already been proposed earlier [5], [6]. We have used the model presented in [7] in order to simulate eddy currents, in general, and induction heating in particular, of ferrous regions. This model gives the dissipated mean power and also the apparent power defined as the product of the RMS values of the current and the voltage.

B. Transient thermal model

The transient thermal computation is realized only on a sub-domain of the magneto-harmonic one. The equations solved are written as shown [8]:

$$\begin{aligned} \operatorname{div}\left(-k \overrightarrow{\operatorname{grad}} \theta\right)+\rho C_p \frac{\partial \theta}{\partial t} &=q \\ k \overrightarrow{\operatorname{grad}} \theta \cdot \vec{n} &=-h\left(\theta-\theta_a\right)-\varepsilon \sigma\left(\theta^4-\theta_a^4\right)+q_s \end{aligned} \quad (4)$$

where the thermal sources q and q_s correspond respectively to the volume and surface power density of eddy currents.

C. Linking or coupling ?

Two ways are possible to solve magneto-thermal problems, that means to connect the magneto-harmonic computation to the transient thermal one : the linking and the coupling.

In the linking way, we first solve the magneto-harmonic problem. We extract the Joule power density and introduce it in the transient thermal problem. We then solve the thermal problem with constant power source with time. In this case, we cannot take into account the variations of the electrical properties with the temperature. For example, the study of the induction heating of ferrous pieces with passing through Curie temperature is impossible. On the other hand, this way is faster because the magneto-harmonic computation is more time expensive than the transient thermal one. We then can approximate the heating through the Curie point by linking with two magneto-harmonic problems, a non linear one below Curie and a linear one above Curie.

In the weak coupling way, magneto-harmonic and transient thermal problem are solved alternatively at each time step of the transient thermal problem. In this case, we can take into account the thermal variations of the electric properties in the magneto-harmonic problem at each time step and so actualise the power sources in the transient thermal problem. This method requires a long computation time when solving a non linear magnetic and non linear thermal problem.

III. 3D PHYSICAL MODELS

A. MF induction heating model

The physical model used for studying a MF induction heating is a cylindrical tube of magnetic steel, external diameter 100 mm, thickness 5 mm, length 300 mm, surrounded by a 12 turns coil, internal diameter 150 mm, length 300 mm. The tube is covered inside and outside by a

thermal insulation so that we can neglect the thermal losses during the heating.

The inductor is supplied by a MF thyristor inverter working at 2.5 kHz. In this case, the skin depth in the tube is closed to 1 mm in the magnetic state, and 11 mm in the non magnetic state. Because of the axi-symmetry property, the 3D computation domain, Fig. 1, contains only a sector of the physical model.

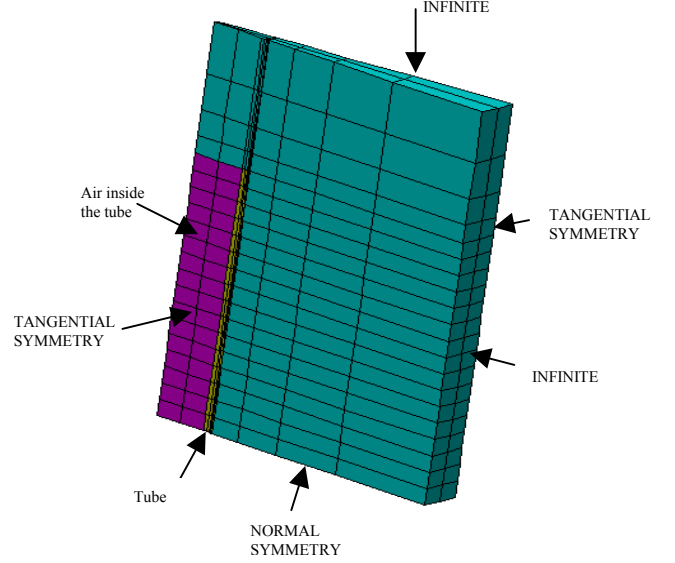


Fig. 1 : 3D computation model, mesh and boundary conditions for the MF induction heating

B. HF induction heating model

The physical model used for the study of HF induction heating, Fig. 2, is a cylindrical tube of magnetic steel with a longitudinal slot. This geometry approximates the pressure welding of tubes using induction heating [9]. A 5 mm slot is realized in the 100 mm outer diameter and 5 mm thickness tube. A 2 turns coil is surrounding the tube in the slitting part and a ferrite made magnetic core is placed inside the tube from the coil to the welding point.

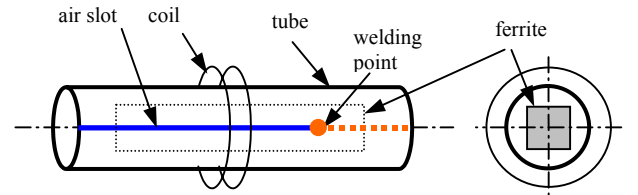


Fig. 2 : Physical model of HF induction heating

A HF IGBT transistor inverter working at 50 kHz supplies the inductor. In this case, the skin depth is closed to 0.5 mm in the magnetic state and 2.5 mm in the non magnetic state. N. Aymard [10], [11], has demonstrated that the surface impedance formulation is available in the magnetic state but not in the non magnetic state. Nevertheless, we extended its

use over Curie point, considering that only a small part of the tube (few millimetres) on both sides of the slot will exceed the Curie temperature.

IV. THE MAGNETO-THERMAL LINKING

A. The MF simulation

Four steps are necessary to study the tube heating from the room temperature to 1,000 °C ; this corresponds to the two states of the steel : the magnetic state below Curie and the non magnetic state above Curie.

The first step is the non linear magneto-harmonic computation. The chosen physical properties are a resistivity of $51.2 \cdot 10^{-8} \Omega \cdot m$, the saturation magnetisation of 1.9 T and an initial slope of the magnetic curve of $100 \cdot \mu_0$. A 6 kA total inductor current at 2.5 kHz supplies the inductor. The total power dissipated in the tube is equal to 19.23 kW.

In the second step, the resulting power density chart is linked to the transient thermal computation. All numerical applications in section IV use the following models for thermal properties of the tube temperature dependent :

- isotropic, exponential variation of thermal conductivity expressed by formula : $15 \cdot \exp^{-T/300} + 25 \text{ J/m}^3/\text{°C}$,
- gaussian model of specific heat, with energy of phase transition $5 \cdot 10^8 \text{ J/m}^3$, temperature of phase transition 760 °C, gaussian standard deviation 100 °C, value 0 °C, $4 \cdot 10^6 \text{ J/m}^3/\text{°C}$

The boundary condition corresponds to no thermal exchange. The simulation stops when the maximum of the tube temperature reaches Curie point.

The third step is the linear magneto-harmonic computation. The chosen physical properties are a resistivity of $90.4 \cdot 10^{-8} \Omega \cdot m$ and a relative permeability of 1. The supply does not change. The total power dissipated in the tube is equal to 7.07 kW.

In the last step, the new power density chart is linked to the transient thermal computation. The boundary conditions corresponds to no thermal exchange and the initial conditions,

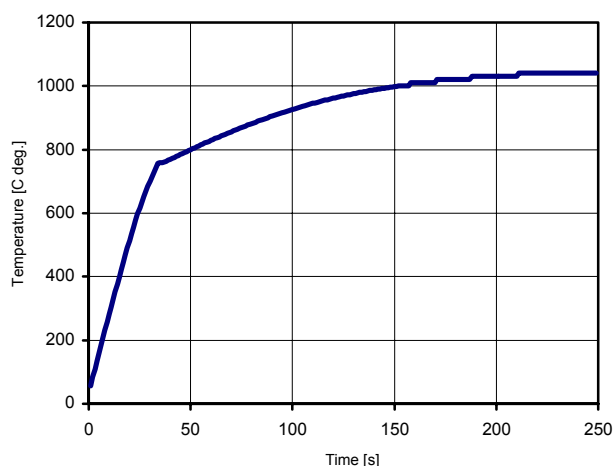


Fig. 3 : Evolution of the tube temperature, magneto-thermal linking, MF

to the temperature chart obtained at the end of the second step.

Figure 3 shows the time evolution of the temperature on the outer surface of the tube in the middle of its length. We have compared the 3D computation with the 2D one using the same linking strategy. The two results are practically identical.

B. The HF simulation

For the HF induction heating application we have used the same linking strategy as earlier to take into account the Curie point crossing. The inductor is supplied by a 1.2 kA total inductor current at 50 kHz. In this case, we have used the non linear surface impedance formulation in the magnetic problem for the first step, and the linear one for the third one.

Before the Curie point, the total power dissipated in the tube is equal to 15.05 kW. After Curie it falls to 2.83 kW. The Figure 4 shows the time evolution of the temperature at the outer surface near the welding point. We can see a sudden drop of the temperature just at the beginning of the second state. This does not happen in the reality because the magnetic state of all the tube does not change suddenly.

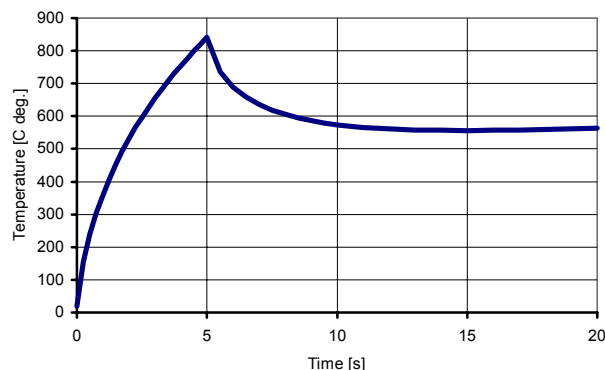


Fig. 4 : Evolution of welding point temperature, magneto-thermal linking HF

This example shows that, in many applications, the simulation of induction heating by linking magneto-harmonic with transient thermal may conduct to wrong results.

V. THE MAGNETO-THERMAL COUPLING. EXPERIMENTAL VALIDATIONS

A. The MF simulation

In the magneto-thermal coupling, we solve alternatively a magneto-harmonic problem and a transient thermal problem. At each thermal time step, we can update the electromagnetic properties in the magnetic problem and the resulting power sources in the thermal one. The variation of electrical properties are as follows: $50 \cdot 10^{-8} (1 + 0.001 \cdot \theta) \Omega \cdot m$ for the resistivity, 2.1 T for saturation magnetisation, 1000 for initial relative permeability, 760 °C for Curie point and 100 °C for time constant of temperature coefficient. That means that the magnetic problem is non linear and we evaluate the volumic distribution of the power density dissipated.

The experimental validation of MF induction heating was

performed on a cylindrical tube of magnetic steel, external diameter 100 mm, thickness 4 mm, length 300 mm, surrounded by a 12 turns coil, internal diameter 150 mm, length 300 mm. The tube is covered by a thermal insulation, so that we neglect the thermal losses during the heating. The inductor was supplied with $275 \times 12 = 3300$ A total current and 2.75 kHz. During the experiment, the values of the current and the frequency were varying with time. For the simulation we have chosen the mean values.

As in the former section, we have realised a 2D and a 3D computation and compared their results with the experiments.

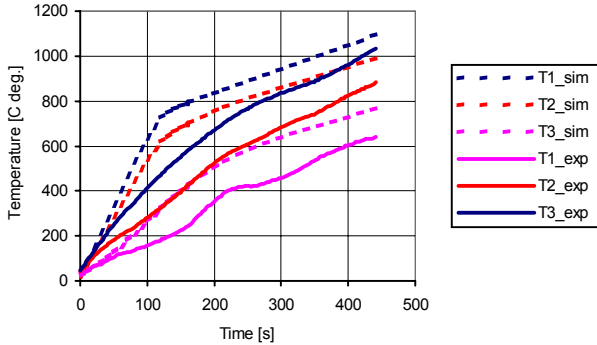


Fig. 5 : Evolution of the tube temperature for MF heating. Comparison with the 2D coupling model

Figure 5 represents the comparison with the 2D model of the evolution of the temperature at three points on the outer surface. It shows some differences between the model and the experiments. Perhaps some physical properties, electrical or thermal are not completely representative.

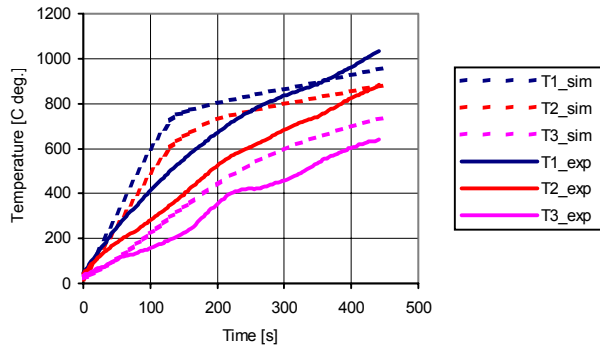


Fig. 6 : Evolution of the tube temperature for MF heating. Comparison with the 3D coupling model

The 3D results, Fig. 6, seem to be closer to the experiment. Nevertheless, we only used first order elements, because algorithm convergence has not been obtained yet with second order elements. In fact, the experience of the previous results shows that the power obtained with second order elements is a little greater. At the end of the heating, the temperature distribution appears as follows (Fig. 7) :

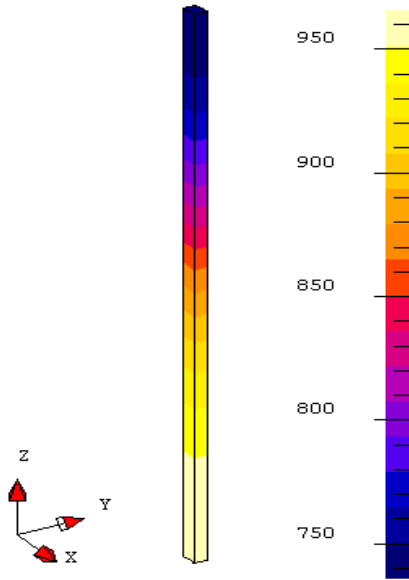


Fig. 7 : Chart of temperature at the end of the heating

B. The HF simulation and experimental validation

Due to the high frequency, we must use a surface impedance formulation to determine the eddy currents in the tube. Now, the software can take into account either temperature variation or magnetic field variation of the surface impedance but not the two parameters simultaneously.

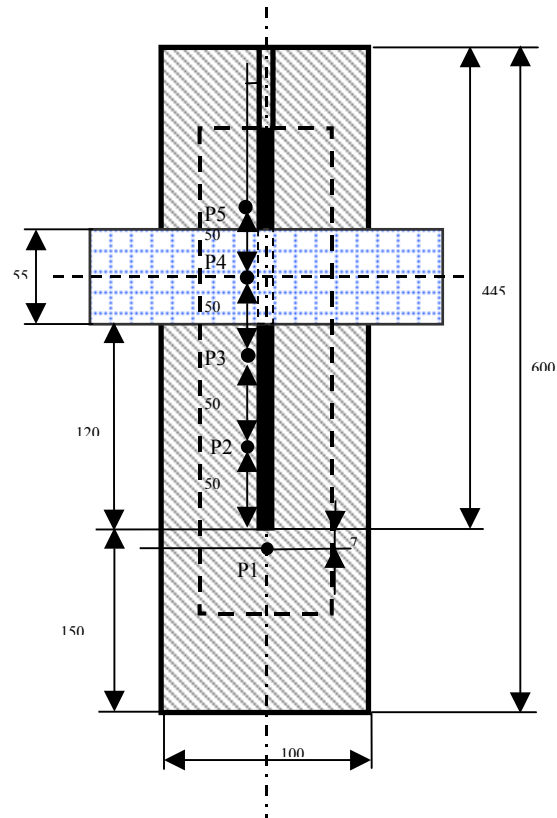


Fig. 8 : Position of the thermocouples in the HF experiment

The variation of electrical properties used for the simulation are as follows : $20 \cdot 10^{-8}(1 + 0.004 \cdot \theta) \Omega \cdot m$ for the resistivity, 750 for tube relative permeability (constant value before Curie), 760 °C for Curie point and 100 °C for time constant of temperature coefficient. That means that, at each time step, the magnetic resolution is linear.

The experimental validation was performed using the tube already described in section III.B. The inductor was supplied with $600 \times 2 = 1200$ A total current and 45 kHz ; the ferrite core has a relative permeability of 50. The thermal losses on all surfaces of the tube during the heating are characterised by the value $20 \text{ W/m}^2/\text{°C}$ for thermal convection and 0.8 for radiation coefficient. Figure 8 shows the positions P1 to P5 of the thermocouples welded on the outer surface of the tube.

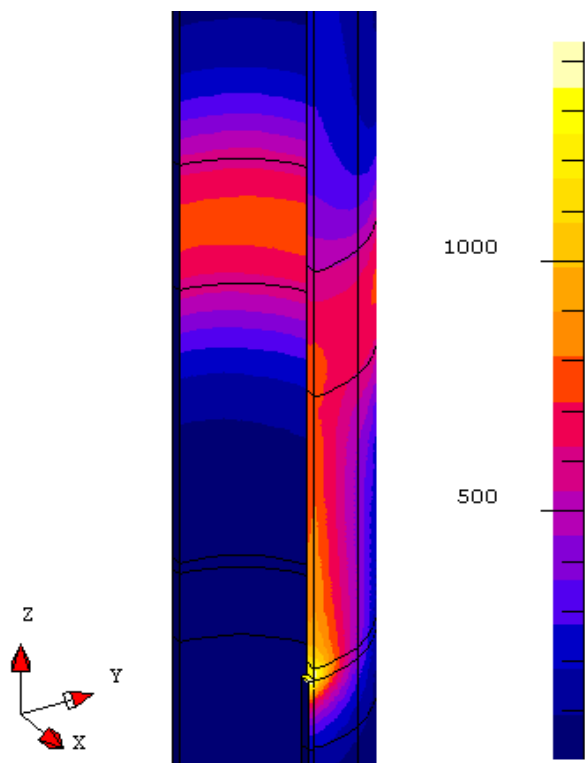


Fig. 9 : Chart of temperature after 40 seconds of HF heating

Figure 9 shows the result of the numerical simulation and represents the temperature chart after 40 seconds of heating. We can see that the heating is concentrated inside the coil and around the slot. The maximal temperature is reached at the welding point.

The evolution of the tube temperature for the five points P1 to P5 is drawn Fig 10. We can see that the welding point P1 reaches the melting temperature (about 1,550 C deg.). Because we have not taken into account the transition energy solid-liquid, P1 temperatures are not valid over 70 s.

The experimental results have been compared with these computed data (Fig. 11). We can see a relative good agreement between the two results. As in the former section, we can suppose that the physical properties are not representative. This is especially true for the magnetic

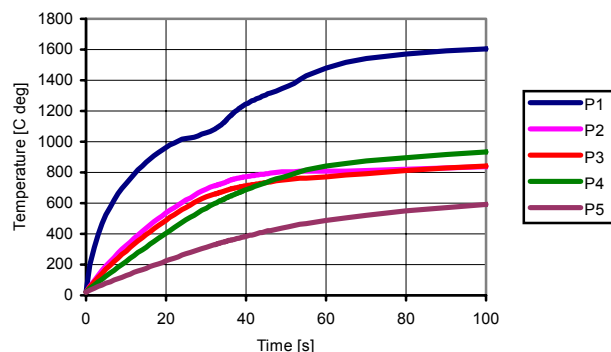


Fig. 10 : Evolution of the tube temperature for HF heating. 3D coupling model

permeability. Inside the coil and around the slot, the metal is very saturated (μ_r small) and not anywhere else. We can see some differences in the evaluation of the induced power with the approach section IV. B. where we used non linear surface impedance.

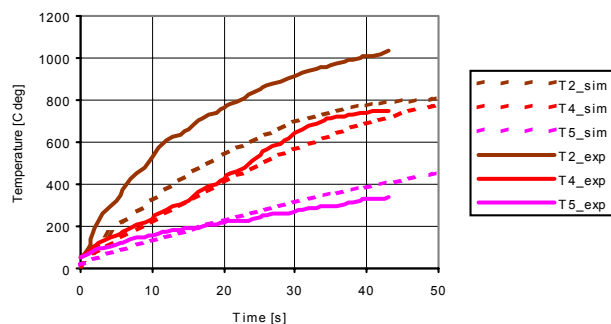


Fig. 11 : Evolution of the tube temperature for HF heating. Comparison between 3D coupling model and experiment

VI. CONCLUSION

This study has shown the advantages and the drawbacks of the coupling way compared to the linking way. The linking way may be profitable when the electrical properties are slightly dependent on the temperature because the computation time is strongly reduced. Otherwise, for example when crossing over Curie temperature, the coupling way is the only one which can give acceptable results. To be in good agreement with experiment, it is also necessary to put more accurate physical properties at different temperatures to describe the behaviour of the material correctly.

New developments will be done to determine an acceptable way to describe the variations of the surface impedance with both the magnetic field and the temperature.

Finally, we are looking for a new strategy for crossing Curie temperature. Because the skin depth varies from 1 to 10, it may be relevant to use a surface formulation below Curie temperature and a volume one above.

REFERENCES

- [1] Y. Du Terrail Couvat, M. Garnier and C. Allemann, "3D parameterised magneto-thermal simulations for modular induction heating devices", *Proc. of EPM2000 International Symposium*, Nagoya, Japan, April 3-6, 2000, pp.
- [2] U. Ludtke and D. Schulze, "FEM software for simulation of heating by internal sources", *Proc. of HIS-01 Int. Seminar*, Padua, Italy, Sept. 12-14, 2001
- [3] Y. Neau, B. Paya, T. Tudorache and V. Fireteanu, "Numerical evaluation and experimental validation of eddy currents and electromagnetic forces in transverse flux induction heating of magnetic steel sheets", *Proc. of EPM2000 International Symposium*, Nagoya, Japan, April 3-6, 2000, pp. 211-217.
- [4] T. H. Fawzi, M. Taher Ahmed and P. E. Burke, "On the use of the impedance boundary condition in eddy current problems", *IEEE Trans. Magn.*, vol. 21, September 1985
- [5] C. Guérin and G. Meunier, "Validation of surface impedance for 3D non linear eddy current problems", *Proc. of CEFC'96*, Okayama, Japan, March 18-20, 1996.
- [6] S. Wanser, L. Krahenbuhl, J. Boule, A. Nicolas : "Computation of 3D Induction heating problems by boundary element, finite element and non-linear surface impedance methods", *Proc. of COMPUMAG 1995*, Berlin, Germany, July 10-13
- [7] B. Paya and C. Guérin, "Magnetic field dependence of non linear surface impedance : Which field to choose ?", *Proc. of COMPUMAG'01*, Évian, France, July 2-5, 2001, *IEEE Trans. Magn.*, Vol.28, N° 2, March 2002, pp. 585-588.
- [8] C. Guérin, "New 3D thermal models", *FLUX Users European Club 2001*, Aix en Provence, France, September 27-28, 2001, CEDRAT.
- [9] H.J. Lessmann : "Calculation of the electromagnetic and thermal processes in inductive longitudinal welding of pipes" , *Elektrowärme International* 51 (1993) B4, November 1993, pp. 186-192
- [10] N. Aymard, "Etude des phénomènes magnétodynamiques pour l'optimisation de structures 3D de chauffage par induction", *PhD dissertation*, Université de Nantes, November 20, 1997
- [11] N. Aymard, M. Feliachi, B. Paya, "An improved modified surface impedance for transverse electric problems", *Proc. of CEFC'96*, Okayama, Japan, March 18-20, 1996.